

1 **Polar amplification as an inherent response of a**
2 **circulating atmosphere: results from the TRACMIP**
3 **aquaplanets**

4 **Rick D. Russotto¹ and Michela Biasutti¹**

5 ¹Lamont-Doherty Earth Observatory of Columbia University

6 ¹61 Route 9W, Palisades, NY 10964

7 **Key Points:**

- 8 • Polar amplification occurs robustly in the TRACMIP aquaplanet simulations
- 9 • Moisture transport mediates the contributions of different forcing and feedback
- 10 components to polar amplification
- 11 • The instantaneous CO₂ forcing and water vapor feedback are the largest contrib-
- 12 utors to polar amplification

Corresponding author: Rick Russotto, russotto@ldeo.columbia.edu

Abstract

In the TRACMIP ensemble of aquaplanet climate model experiments, CO₂-induced warming is amplified in the poles in 10 out of 12 models, despite the lack of sea ice. We attribute causes of this amplification by perturbing individual radiative forcing and feedback components in a moist energy balance model. We find a strikingly linear pattern of tropical versus polar warming contributions across models and processes, implying that polar amplification is an inherent consequence of diffusion of moist static energy by the atmosphere. The largest contributor to polar amplification is the instantaneous CO₂ forcing, followed by the water vapor feedback and, for some models, cloud feedbacks. Extratropical feedbacks affect polar amplification more strongly, but even feedbacks confined to the tropics can cause polar amplification. Our results contradict studies inferring warming contributions directly from the meridional gradient of radiative perturbations, highlighting the importance of interactions between feedbacks and moisture transport for polar amplification.

Plain Language Summary

In both observations and computer model simulations, the polar regions (especially the Arctic) warm more than the rest of the world in response to increased greenhouse gas concentrations. Scientists disagree on the reasons for this “polar amplification” of warming. The melting of ice floating in the ocean, which lets more sunlight be absorbed, is often given as an explanation, but climate models with no sea ice also display polar amplification. We ran hundreds of experiments with a simple climate model in order to understand the reasons for polar amplification in more complex models that lack sea ice. We found that the main reason is that the atmosphere transports energy from the tropics to the poles, so much so that even processes that initially add energy mostly to the tropics cause polar amplification. Our methods produce different explanations from past studies because they did not fully account for this movement of energy.

1 Introduction

Despite many years of research, the causes of the polar amplification of warming caused by increased greenhouse gases remain a topic of debate. This phenomenon of greater warming at the poles is often attributed to feedbacks involving the loss of polar ice, due to the exposure of less reflective underlying surfaces (Hall, 2004; Crook et al., 2011) or

44 interactions between sea ice and ocean heat storage and release (Dai et al., 2019). How-
45 ever, polar amplification has also been found in global climate model (GCM) simulations
46 with fixed albedo (Alexeev et al., 2005; Graversen & Wang, 2009), indicating that ice-
47 albedo feedbacks are not necessary for polar amplified warming. The opposing sign of
48 the lapse rate feedback at low versus high latitudes (Pithan & Mauritsen, 2014; Payne
49 et al., 2015) and cloud feedbacks (Vavrus, 2004) have also been cited as contributing fac-
50 tors to polar amplification.

51 In the context of this body of work, the Tropical Rain belts with an Annual cycle
52 and Continent Model Intercomparison Project (TRACMIP; Voigt et al. (2016)) is well
53 positioned to provide useful insights into polar amplification, as it provides the physics
54 of complex models but a very idealized configuration. TRACMIP consists of aquaplanet
55 GCM experiments with a seasonal cycle, a slab ocean with 30 m mixed layer depth, and
56 a prescribed ocean heat transport in the form of q -fluxes approximating that of the real
57 Earth in the zonal mean. Clouds and water vapor are allowed to interact with atmospheric
58 radiation in all 12 models considered in this study, but there is no sea ice in any of the
59 models. We consider the difference between the AquaControl experiment, with a CO₂
60 concentration of 348 ppmv, and the Aqua4xCO₂ experiment, in which CO₂ is quadru-
61 pled, similar to the Abrupt4xCO₂ experiment of the Coupled Model Intercomparison
62 Project (CMIP; Taylor et al. (2012)). Polar amplification in response to quadrupled CO₂
63 occurs in 10 out of 12 full-radiation GCMs (Fig. 1a,f), making this a useful multi-model
64 test case to attribute the causes of polar amplification in the absence of surface ice.

65 This study aims to account for the polar amplification in the TRACMIP Aqua4xCO₂
66 ensemble, despite the lack of sea ice, and to comment on the behavior of the meridional
67 temperature gradient in GCMs and energy balance models. We attribute the contribu-
68 tions of different radiative feedbacks, rapid adjustments, and the instantaneous CO₂ forc-
69 ing to the polar amplification in TRACMIP. Some studies (Pithan & Mauritsen, 2014;
70 Goosse et al., 2018; Stuecker et al., 2018) have done this attribution by calculating the
71 change in radiation at the top of atmosphere (TOA) from each feedback, then diagnos-
72 ing a surface warming contribution, for example by inverting the surface temperature
73 radiative kernel (Pithan & Mauritsen, 2014) or normalizing by the global mean Planck
74 feedback (Goosse et al., 2018). These studies have typically found that polar amplifica-
75 tion is primarily due to local, high-latitude forcings and feedbacks, particularly the lapse
76 rate feedback, which is positive at high latitudes and otherwise negative, with the sur-

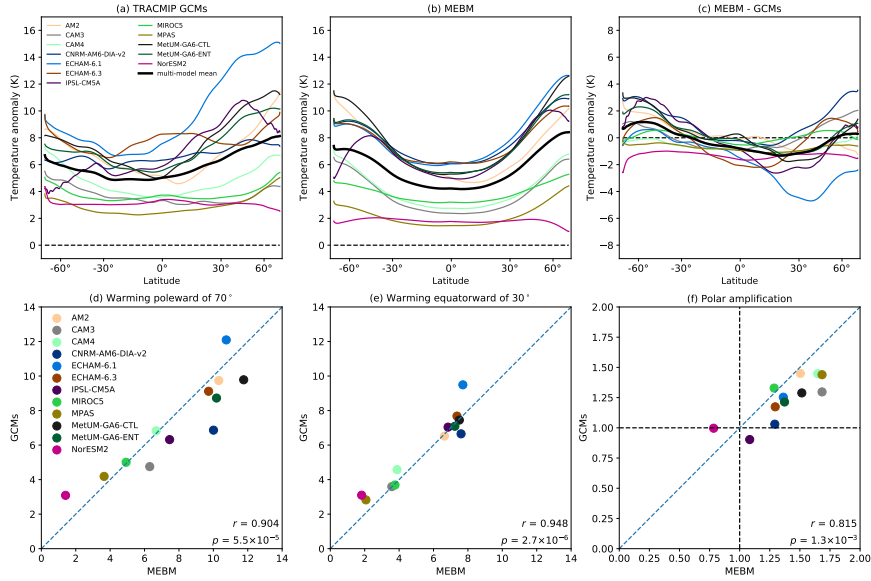


Figure 1. Zonal mean surface temperature change in (a) TRACMIP GCMs, (b) moist energy balance model, and (c) difference, and scatter plots of warming in MEBM vs. GCMs averaged over high latitudes (d), tropics (e), and ratio of high latitude to global mean warming (f). Refer to model names in Table 3 of Voigt et al. (2016). In (d)-(f), r is the correlation coefficient and p is the p -value of a 2-tailed t -test for whether the slope is different from 0. We exclude the Caltech gray radiation GCM because it lacks most of the feedbacks that we consider.

77 face albedo feedback playing a secondary role. Other studies (Rose et al., 2014; Hwang
78 & Frierson, 2010; Hwang et al., 2011; Roe et al., 2015; Bonan et al., 2018; Armour et al.,
79 2019) have run attribution experiments in which forcings and feedbacks are perturbed
80 in a moist energy balance model (MEBM) which allows for interactions between the feed-
81 backs and energy transport. Hwang and Frierson (2010) demonstrated that the MEBM
82 well reproduces poleward energy transport in coupled models, and found cloud feedbacks
83 to be the largest source of inter-model spread. Perturbing the feedback parameter in the
84 MEBM either in the tropics or the poles, either with idealized perturbations (Roe et al.,
85 2015) or with CMIP5-based feedbacks (Bonan et al., 2018), indicates that uncertainty
86 in tropical feedbacks strongly transmits the inter-model spread in warming to the poles,
87 while the effects of polar feedbacks are felt more locally.

88 We apply the MEBM approach to the TRACMIP ensemble, combining different
89 methodologies in a way not previously done to study the roles of specific forcings and
90 feedbacks in enhancing tropical versus polar warming. We show that the roles of var-
91 ious feedbacks, particularly the water vapor feedback, in polar amplification are much
92 different from what has been described in the existing literature when interactions with
93 energy transport are accounted for. We also find striking consistency in the ratio of con-
94 tributions to tropical versus polar warming across models and feedbacks, with positive
95 feedbacks in general causing polar amplification. This suggests that polar amplification
96 of warming is an inherent property of an atmosphere that diffuses moist static energy
97 (MSE), as previously suggested by Merlis and Henry (2018).

98 **2 Methods**

99 **2.1 Setup of moist energy balance model experiments**

100 Energy balance models (EBMs) are one-dimensional representations of the zonal
101 mean climate that diffuse energy down-gradient (e.g., North et al., 1981). MEBMs, first
102 introduced by Flannery (1984), are an extension of classical EBMs and diffuse moist static
103 energy (MSE) rather than temperature. There are two MEBM versions commonly used
104 today: a climatological version, used, *e.g.*, by Hwang and Frierson (2010), Hwang et al.
105 (2011), and Frierson and Hwang (2012), and a perturbation version, used by Rose et al.
106 (2014), Roe et al. (2015), Siler et al. (2018), Bonan et al. (2018), and Armour et al. (2019).
107 The climatological MEBM diffuses absolute MSE and highly simplifies radiative feed-

108 backs. The perturbation MEBM diffuses anomalous MSE and allows feedbacks to vary
 109 with latitude. We use the perturbation MEBM because it allows for independent spec-
 110 ification of LW feedbacks, and because it allows feedbacks to interact with local temper-
 111 ature changes.

112 The diffusion of MSE in the perturbation MEBM, neglecting changes in ocean heat
 113 uptake which do not apply here, is expressed by (*e.g.* Bonan et al., 2018):

$$R_f(x) + \lambda(x)T'_s(x) + \frac{p_s}{a^2g}D\frac{d}{dx}\left[(1-x^2)\frac{dh'(x)}{dx}\right] = 0. \quad (1)$$

114 Here $R_f(x)$ is the effective radiative forcing associated with the CO₂ increase, which is
 115 defined as the instantaneous CO₂ forcing plus the sum of the changes to the TOA en-
 116 ergy balance, known as rapid adjustments, that occur when atmospheric temperature,
 117 humidity, and clouds respond to the CO₂ increase before the sea surface temperature
 118 has a chance to respond (Myhre et al., 2013); x is the sine of latitude; λ is the net ra-
 119 diative feedback; T'_s is the surface temperature anomaly; p_s is the surface pressure; a is
 120 the Earth’s radius; g is the gravitational acceleration; D is the diffusivity; and $h' = c_pT' +$
 121 L_vq' is the perturbation near-surface MSE, where c_p is the heat capacity of air at con-
 122 stant pressure, L_v is the latent heat of vaporization of water, and q' is the perturbation
 123 specific humidity. The MEBM is run to equilibrium starting from a uniform tempera-
 124 ture profile, with specified values of $R_f(x)$ and $\lambda(x)$. We use a value of $9.6 \times 10^5 \text{ m}^2 \text{ s}^{-1}$
 125 for D , following Bonan et al. (2018), and a relative humidity of 80% as is typical for these
 126 experiments. We also tried a diffusivity of $1.06 \times 10^6 \text{ m}^2 \text{ s}^{-1}$, following Hwang and Frier-
 127 son (2010), and found that it did not much affect T'_s at equilibrium (not shown), con-
 128 sistent with the finding of Armour et al. (2019) that varying diffusivity by a factor of 2
 129 had little effect on the MEBM behavior. For our “control” MEBM experiment, we cal-
 130 culate R_f and λ by regressing the total anomaly in top of atmosphere (TOA) radiative
 131 imbalance against the surface temperature anomaly at each latitude in Aqua4xCO₂ -
 132 AquaControl, following Gregory et al. (2004). The slope of this regression is λ , and the
 133 intercept is R_f . Anomalies are calculated in each month of Aqua4xCO₂ relative to the
 134 climatology for that month in AquaControl, and then the mean of each year is taken be-
 135 fore regression to eliminate effects of changes in the seasonal cycle. Note that feedbacks
 136 calculated this way are defined against zonal mean, rather than global mean, temper-
 137 ature change (see Feldl and Roe (2013) for a discussion of this distinction).

138 For each physical property of interest, including cloud cover, humidity, and atmo-
 139 spheric temperature, we calculate the change in TOA radiative flux using established meth-
 140 ods and regress it against surface temperature anomalies using the Gregory method. The
 141 intercept of each regression is the rapid adjustment, or the contribution to the effective
 142 radiative forcing, and the slope is the feedback. We calculate rapid adjustments and feed-
 143 backs for different physical processes in each TRACMIP model individually, then “turn
 144 off” each of them one at a time in the perturbation MEBM by subtracting each rapid
 145 adjustment from R_f and subtracting each feedback from λ . The effect of turning off each
 146 process on the meridional temperature gradient, relative to a control MEBM run forced
 147 with the effective radiative forcing and total radiative feedback, represents the contri-
 148 bution of that process to polar amplification (with the sign reversed). Note that turn-
 149 ing off the atmospheric temperature feedback (Planck plus lapse rate) results in a run-
 150 away greenhouse effect due to a positive total feedback, so instead we reduce the strength
 151 of this feedback by 10%. Perturbing the feedback by 5% and 15% instead results in an
 152 overall warming that scales exponentially with the amount reduced (not shown), but the
 153 ratio of polar to tropical differences in T'_s is similar in all three cases.

154 In its control configuration, the perturbation EBM exhibits a pattern of warming
 155 amplified at the poles similar to that seen in the GCMs themselves, albeit the MEBM
 156 warming is smoother and more hemispherically symmetric (Figure 1b-c). There are strong
 157 correlations, with correlation coefficient r at least 0.81, between the MEBM- and GCM-
 158 derived warming averaged over high latitudes (poleward of 70° ; Figure 1d), the tropics
 159 (equatorward of 30° ; Figure 1e), and for the polar amplification (warming poleward of
 160 70° divided by global mean warming, following Hwang et al. (2011); Figure 1f). These
 161 correlations are all statistically significant at the 1% level. The good agreement between
 162 the MEBM and GCMs shown in Figure 1 gives us confidence that attribution experi-
 163 ments in which rapid adjustments and feedbacks are perturbed individually in the MEBM
 164 will tell us something useful about the causes of polar amplification in the TRACMIP
 165 ensemble.

166 **2.2 Calculation of instantaneous forcing, rapid adjustments, and feed-** 167 **backs**

168 Different methods are used to calculate the SW and LW perturbations to the TOA
 169 energy balance, in W m^{-2} , associated with different physical processes, which are then

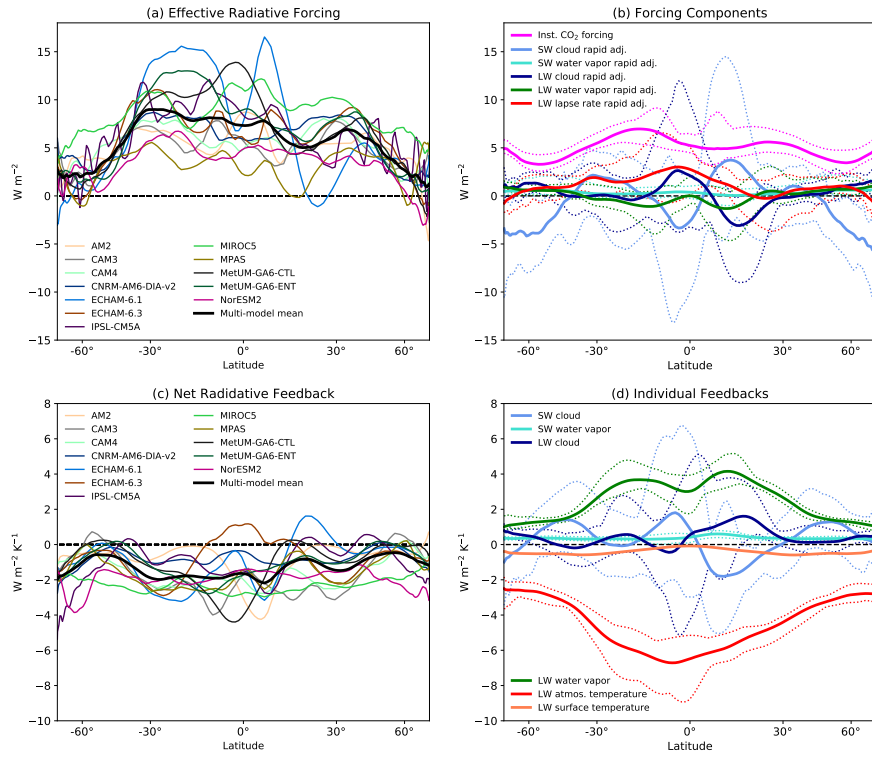


Figure 2. (a) Effective radiative forcing in each TRACMIP model. (b) Individual rapid adjustments and instantaneous CO_2 forcing: multi-model mean (solid curves) and maximum and minimum models (dotted curves in same colors). (c) Net radiative feedback in each TRACMIP model. (d) As in (b) but for individual radiative feedbacks. Forcing and feedback components for individual models are shown in Figure S2.

170 regressed against surface warming on a latitude-by-latitude basis to obtain radiative ad-
171 justments and feedbacks. This process is summarized in a flowchart in Figure S1. For
172 the SW, we use the Approximate Partial Radiation Perturbation method (APRP; Taylor
173 et al. (2007)) to calculate the radiative effects of changes in cloud properties and in non-
174 cloud atmospheric scattering and absorption. The latter is mainly due to SW absorp-
175 tion by water vapor, so we refer to this as the SW water vapor adjustment and feedback.
176 For the LW, we use the all-sky aquaplanet radiative kernels developed by Feldl et al. (2017)
177 to calculate the rapid adjustments and feedbacks associated with atmospheric temper-
178 ature (including Planck and lapse rate effects), surface temperature, and water vapor.
179 We calculate the LW radiative effects of changes in cloud properties by first calculating
180 the change in the LW cloud radiative effect (the difference in outgoing longwave radi-
181 ation between all-sky and clear-sky conditions), and then subtracting out the contribu-
182 tions of pre-existing clouds to the other forcing and feedback components, which we ob-
183 tain using the difference between the clear-sky and all-sky versions of the radiative ker-
184 nels, following Shell et al. (2008) and Soden et al. (2008). Finally, after running Gregory
185 regressions for the total perturbation and for each physical process, we estimate the in-
186 stantaneous CO₂ radiative forcing by subtracting the sum of the rapid adjustments from
187 the effective forcing.

188 The effective radiative forcing and its components are shown in Figure 2a and 2b,
189 respectively. The effective radiative forcing is largest between 30°S and 30°N and de-
190 cays towards the poles. This qualitative behavior is consistent across models, though inter-
191 model range is large. The physical reason for this pattern can be inferred from the in-
192 dividual components (Figure 2b). The instantaneous CO₂ forcing is relatively uniform
193 across latitudes and has relatively little spread. The rapid adjustments are small by com-
194 parison to it, but exhibit much inter-model spread, particularly for the cloud adjustments.
195 The SW cloud adjustment is negative in the poles for all models, resulting in the effec-
196 tive radiative forcing being weaker in the high latitudes than in the tropics.

197 The net feedback parameter (Figure 2c) is quite constant in latitude in the multi-
198 model mean, but some individual models simulate a much more complex structure, with
199 latitudinal differences of about 4 W m⁻² K⁻¹. Among the individual feedbacks (Figure
200 2d), the water vapor feedback is consistently positive in all models, and stronger in the
201 tropics, with the LW component being an order of magnitude stronger than the SW. The
202 SW and LW cloud feedbacks vary in sign with latitude, and tend to be anticorrelated

203 with each other; they are positive in the multi-model, global mean, but the inter-model
204 spread surrounds zero at most latitudes and often exceeds that of the total net radia-
205 tive feedback. The LW atmospheric temperature feedback, which includes the Planck
206 and lapse rate feedbacks, is strongly negative, more so in the tropics. We decomposed
207 the atmospheric temperature feedback into the Planck and lapse rate components (not
208 shown), but since turning each component off in the MEBM caused a runaway feedback
209 for at least half the models, we limited our analysis to a 10% reduction in the total at-
210 mospheric temperature feedback. The surface temperature rapid adjustment is 0 by def-
211 inition, and the surface temperature feedback reduces to the kernel, so it has no inter-
212 model spread. However, we can still consider the effect of this weakly negative feedback
213 on the multi-model mean response.

214 **3 Results**

215 Figure 3a,b shows the multi-model mean equilibrium temperature in each MEBM
216 perturbation experiment. The rapid adjustments (Figure 3a) generally have less of an
217 effect on the temperature change than the corresponding feedbacks (Figure 3b). On the
218 other hand, turning off the instantaneous CO₂ forcing, leaving only the rapid adjustments
219 to force the MEBM, completely eliminates the polar amplification (gray curve in Fig-
220 ure 3a). Polar amplification occurs in all of the feedback perturbation experiments, but
221 it is weakened when the water vapor feedbacks are removed. Feedbacks involving clouds,
222 which vary in sign with latitude, have the smallest effect on temperature in the multi-
223 model mean.

224 The bottom 6 panels of Figure 3 show the contribution to warming at each lati-
225 tude from each rapid adjustment, feedback, and the instantaneous forcing, obtained by
226 taking the difference in the temperature anomaly from the control case and flipping the
227 sign. As noted above, completely turning off the atmospheric temperature feedback would
228 result in runaway warming, so the word “contribution” should not be taken literally in
229 the case where this feedback is reduced by 10%. For the rapid adjustments (Figure 3c-
230 3e), the inter-model spread is fairly small, but the cloud rapid adjustments might have
231 an appreciable effect on polar amplification towards the edges of the model envelope. The
232 instantaneous CO₂ forcing (Figure 3e) consistently contributes to polar amplification.
233 Both the SW and LW cloud feedbacks (Figure 3f) have great inter-model uncertainty
234 in their effect on polar amplification; they could either contribute to or detract from it

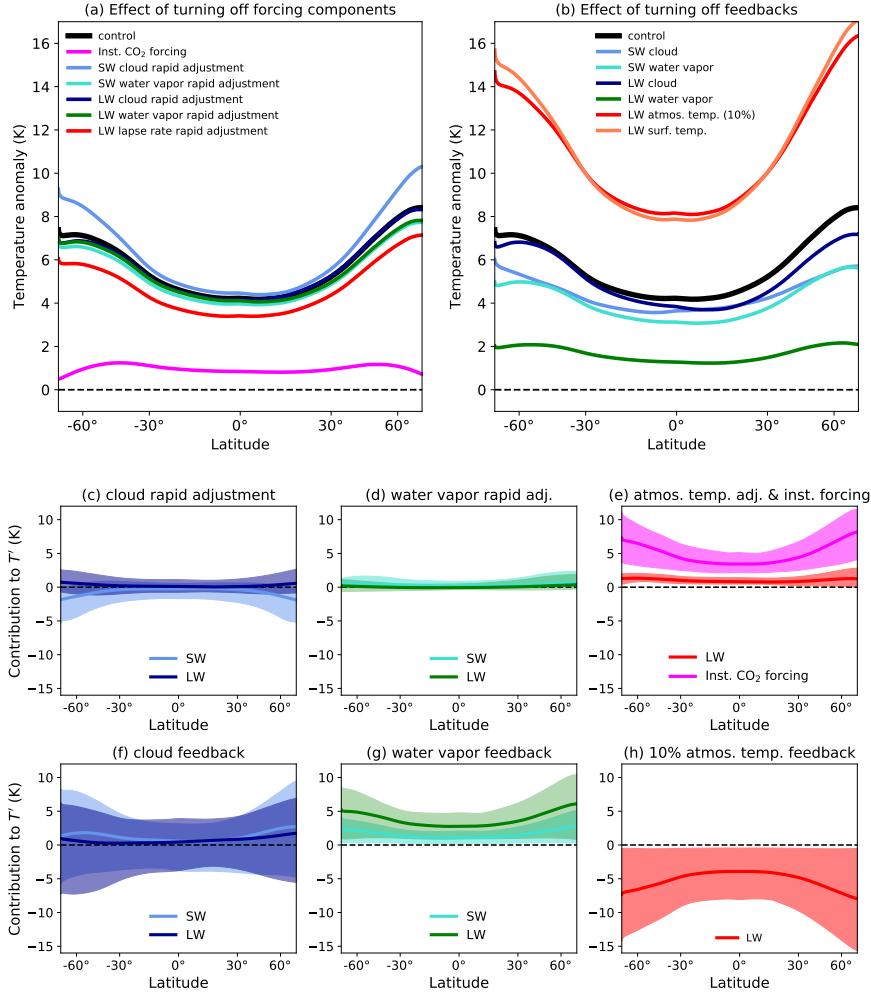


Figure 3. (a-b): Multi-model mean, MEBM-derived equilibrium zonal mean temperature anomalies in the control case (black) and perturbation experiments (colors). (c-h): Warming contribution associated with each forcing or feedback component (negative of the difference in warming from control), in the multi-model mean (curves) and range between maximum and minimum models (shaded areas). Warming contributions for individual models are shown in Figure S3.

235 depending on whether they cause overall warming or cooling. The water vapor feedback
236 (Figure 3g), especially in the LW, tends to contribute to polar amplification, while the
237 10% perturbation of the atmospheric temperature feedback (Figure 3h), and similarly
238 the surface temperature feedback (not shown), act in opposition to polar amplification
239 by causing more cooling at the poles. In a couple of models, however, these latter two
240 feedbacks have weak effects on both overall warming and polar amplification (see Fig-
241 ure S3). The positive and negative contributions to polar amplification by the water va-
242 por and atmospheric temperature feedbacks, respectively, are counterintuitive, as these
243 feedbacks are stronger in the tropics than at the poles (Figure 2d).

244 To further investigate the roles of the different rapid adjustments and feedbacks
245 to tropical versus polar warming, Figure 4a shows a similar style of scatter plot to Fig-
246 ure 1 of Pithan and Mauritsen (2014), with contributions to tropical (30°S-30°N) warm-
247 ing on the x -axis and contributions to polar (poleward of 70°) warming on the y -axis.
248 Points above the 1:1 diagonal (pink background) indicate greater polar than tropical warm-
249 ing, *i.e.* the process contributes to polar amplification, while points below the diagonal
250 (blue background) indicate processes that detract from polar amplification.

251 The most striking feature of Figure 4a is how linear the points are. A regression
252 of the polar against the tropical warming contribution for each of the individual model-
253 experiment pairs (shown as small symbols) has a very strong correlation, $r > 0.98$, with
254 a least-squares best fit line (dashed) being steeper than the 1:1 line and passing very close
255 to the origin. Very few points showing enhanced overall warming lie below the 1:1 line,
256 while very few points showing diminished overall warming lie above it. Physically, this
257 means that positive rapid adjustments and feedbacks contribute to polar amplification,
258 while negative rapid adjustments and feedbacks oppose polar amplification. We can iden-
259 tify which processes contribute most strongly to polar amplification by looking at how
260 far the multi-model means (large symbols) lie above the 1:1 line. The strongest contrib-
261 utor is the instantaneous CO₂ forcing, suggesting that polar amplification is an inher-
262 ent response of the atmosphere to positive forcing and not primarily caused by any in-
263 dividual feedback or rapid adjustment. The strongest positive feedback—the LW water
264 vapor feedback—is the next largest contributor, followed by the SW water vapor feed-
265 back, and the SW and LW cloud feedbacks, although the cloud feedback contributions
266 might be on par with that of the water vapor feedback, or negative, depending on the
267 model. The surface and atmospheric temperature feedbacks, and the SW cloud rapid ad-

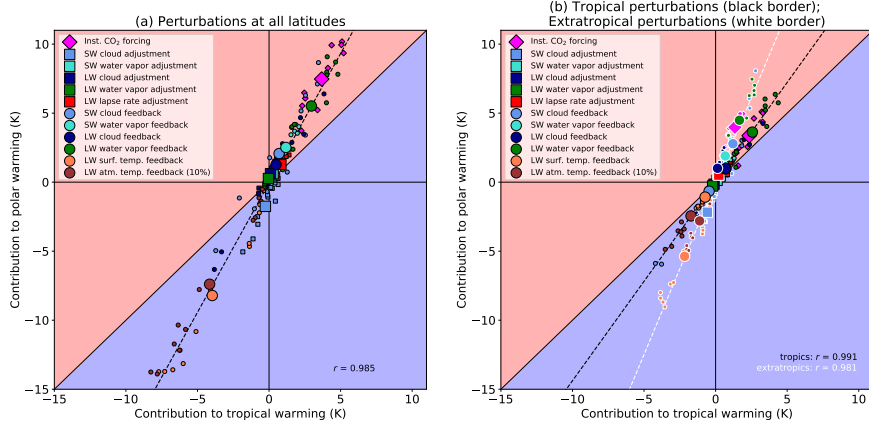


Figure 4. Contributions of each rapid adjustment, feedback, and the instantaneous CO₂ forcing to tropical (equatorward of 30 degrees) warming (x axis) and polar (poleward of 70 degrees) warming (y axis), for global (a) or tropical vs. extratropical (b) forcing and feedback perturbations. Large symbols are multi-model means; small symbols are results for individual models. Least squares regression fit lines (dashed) and correlation coefficients (r) calculated from the full set of runs from each model and experiment. Results for individual models are shown in Figures S4 and S5.

268 justment, work against polar amplification in TRACMIP (but see the above caveat about
 269 the magnitude for the atmospheric temperature feedback). A 1-dimensional chart show-
 270 ing contributions to polar amplification is shown in Figure S6.

271 To help answer the question of whether local or nonlocal feedbacks are more im-
 272 portant for polar amplification, we ran additional sets of MEBM experiments in which
 273 perturbations to R_f or λ were made only in the tropics (equatorward of 30°) or extra-
 274 tropics (poleward of 30°); these regions were chosen for simplicity and equal area. Con-
 275 tributions to tropical versus polar warming for these MEBM runs are shown in Figure
 276 4b, with the tropical perturbation results having black symbol edges and the extratrop-
 277 ical having white edges. The impacts on overall warming are smaller than in Figure 4a,
 278 expected given the smaller overall perturbations being applied, but each set of exper-
 279 iments still has a very linear set of responses, again with $r > 0.98$. The slope is steeper
 280 for the extratropical perturbations, indicating that feedbacks there more strongly effect
 281 polar amplification, consistent with Roe et al. (2015) and Stuecker et al. (2018). But,
 282 with the exceptions of 2 models (Figure S5), positive feedbacks and forcing components

283 still usually contribute to polar amplification even when only their tropical components
284 are considered, with the slope being greater than the 1:1 line at the 1% significance level.
285 Other studies that have applied CO₂ forcing only in the tropics have been more ambigu-
286 ous, producing polar amplification only in the Arctic (Stuecker et al., 2018) or only in
287 one of two aquaplanet models (Shaw & Tan, 2018), perhaps because their tropical per-
288 turbations were narrower than ours, extending only 10 or 20 degrees from the equator,
289 respectively. Still, the fact remains that such tropical perturbations do not lead to strongly
290 tropical amplified warming, and in some models can even cause polar amplification. There-
291 fore, analyses that presume to explain whether a forcing or feedback enhances or dimin-
292 ishes polar amplification on the sole basis of whether it is stronger in the tropics or poles
293 could be profoundly misleading if their limitations are not considered carefully.

294 4 Discussion

295 The TRACMIP ensemble demonstrates that an ice-albedo feedback is not neces-
296 sary to obtain polar amplification in most models in a GCM ensemble. Moreover, we have
297 identified the instantaneous CO₂ forcing as the strongest contributor accounting for the
298 existence of polar amplification in the ice-free TRACMIP ensemble, followed by the wa-
299 ter vapor feedback, with SW and LW cloud feedbacks also being important for some mod-
300 els. These amplifying factors work in opposition to a Planck feedback that weakens po-
301 lar amplification. The lapse rate feedback, which is negative at low latitudes but pos-
302 itive at high latitudes, may have a contribution to polar amplification which our meth-
303 ods could not identify, but in any case, this effect is masked by the always negative Planck
304 feedback. The fact that the Caltech gray radiation model (O’Gorman & Schneider, 2008;
305 Bordoni & Schneider, 2008), which lacks most of the physical processes responsible for
306 the rapid adjustments and feedbacks, also exhibits polar amplification in TRACMIP (Voigt
307 et al., 2016) further points to the primary role of the instantaneous CO₂ forcing in po-
308 lar amplification, although this model does have a spatially varying lapse rate feedback
309 that appears to contribute to polar amplification in a framework that does not consider
310 interactions with energy transport (Henry & Merlis, 2019).

311 It would be useful to use similar MEBM perturbation methods to break down the
312 individual feedback contributions to polar amplification in a fully coupled GCM ensem-
313 ble; we suspect that the water vapor feedback would still be found to have a positive con-
314 tribution to polar amplification when considered this way, but the ice albedo feedback

315 would also be important because it is positive and focused in high latitudes. The polar
316 amplification in TRACMIP, while robust, is, at ≤ 1.5 (Figure 1f), much weaker than
317 in the fully coupled CMIP5 equivalent (Figure S7), and ice-albedo feedback likely helps
318 explain this difference in magnitude. Of course, even the fully coupled CMIP5 models
319 have difficulty simulating some processes important to high latitude climate (e.g. Turner
320 et al., 2015; Jones et al., 2016), so higher-resolution regional models will also continue
321 to be important in understanding the interactions between ice and polar temperatures.

322 Our results, particularly regarding the role of the water vapor feedback, contradict
323 those of past attempts to diagnose the causes of polar amplification. Studies making sim-
324 ilar scatter plots to those in Figure 4 (Pithan & Mauritsen, 2014; Goosse et al., 2018;
325 Stuecker et al., 2018) all describe the water vapor feedback as opposing polar amplifi-
326 cation. Since these studies assume a 1:1 correspondence between TOA radiative changes
327 and surface warming contributions, they do not account for interactions between radia-
328 tive feedbacks and local temperature or MSE transport, and neglecting these interac-
329 tions has previously been shown to affect inferred contributions to polar amplification
330 (Merlis, 2014). On the other hand, Graversen and Wang (2009) cited the water vapor
331 feedback as a reason for polar amplification in GCM experiments with fixed albedo, and
332 our results support this conclusion. To further investigate energy transport interactions,
333 we have run an alternative set of EBM experiments in a configuration that diffuses only
334 dry static energy. This eliminates the polar amplification in the control case (Figure S8),
335 and the water vapor radiative feedback now opposes polar amplification in the multi-
336 model mean (Figure S9), indicating that latent heat transport plays a critical role in po-
337 lar amplification and in the effect of individual feedbacks on it. The complexity of these
338 interactions illustrates that energy transport should not be thought of as an indepen-
339 dent contributor to polar amplification to be considered separately from individual cli-
340 mate feedbacks.

341 Eliminating the moisture transport recaptures some of the north-south warming
342 asymmetry seen in the GCMs (*cf.* Figures 1 and S8), suggesting that the MEBM misses
343 some important aspects of the warming pattern by diffusing too much latent heat out
344 of the tropics in both directions. The MEBM also neglects effects of the vertical struc-
345 ture of forcings and feedbacks on surface temperature change that have been found to
346 be important in single column models (Payne et al., 2015) and analytic calculations (Cronin
347 & Jansen, 2016). More generally, the very strong linearity shown in Figure 4 might seem

348 “too good to be true”, suggesting we should be cautious about extrapolating results from
349 such a simple model to the real, vastly more complex Earth. These caveats motivate the
350 possibility of applying similar “mechanism denial” methods to study polar amplification
351 in a more comprehensive GCM context. Others have already perturbed individual forc-
352 ings and feedbacks in comprehensive GCMs to study polar amplification, such as apply-
353 ing CO₂ forcing in specific latitude bands (Stuecker et al., 2018), or eliminating the ice-
354 albedo feedback (Alexeev et al., 2005; Graverson & Wang, 2009), interactivity of sea ice
355 with the ocean (Dai et al., 2019), or cloud-radiation interactions (Stevens et al., 2012).
356 A multi-GCM study perturbing *all* relevant feedbacks would be a major and difficult un-
357 dertaking, but it might help to resolve the disagreements over the causes of polar am-
358 plification obtained from limited GCM experiments and different diagnostic techniques.

359 **Acknowledgments**

360 The authors and the TRACMIP project are supported by NSF award AGS-1565522. We
361 thank the referees, Tim Merlis and one anonymous reviewer, for their helpful comments
362 on this manuscript. We thank Nicole Feldl for assistance with using the aquaplanet ra-
363 diative kernels and Lorenzo Polvani for helpful discussions. We acknowledge the work
364 of the TRACMIP modelers (listed in Voigt et al. (2016)) in generating, curating, and
365 making available the model output. The TRACMIP output has been uploaded to the
366 Earth Science Grid Federation repository at [https://esgf-data.dkrz.de/search/esgf-
367 -dkrz/](https://esgf-data.dkrz.de/search/esgf-dkrz/), in a format consistent with the Climate Model Output Rewriter conventions.
368 IPython notebooks used to analyze data and make plots are uploaded to [https://github
369 .com/rdrussotto/TRACMIP_pa_notebooks](https://github.com/rdrussotto/TRACMIP_pa_notebooks). These will be transferred to a permanent repos-
370 itory upon acceptance of the paper.

371 **References**

- 372 Alexeev, V. A., Langen, P. L., & Bates, J. R. (2005). Polar amplification of surface
373 warming on an aquaplanet in “ghost forcing” experiments without sea ice feed-
374 backs. *Climate Dynamics*, *24*(7), 655–666. doi: 10.1007/s00382-005-0018-3
- 375 Armour, K. C., Siler, N., Donohoe, A., & Roe, G. H. (2019). Meridional atmospheric
376 heat transport constrained by energetics and mediated by large-scale diffusion.
377 *Journal of Climate*, *32*(12), 3655–3680. doi: 10.1175/JCLI-D-18-0563.1
- 378 Bonan, D. B., Armour, K. C., Roe, G. H., Siler, N., & Feldl, N. (2018). Sources of

- 379 uncertainty in the meridional pattern of climate change. *Geophysical Research*
380 *Letters*, *45*(17), 9131-9140. doi: 10.1029/2018GL079429
- 381 Bordoni, S., & Schneider, T. (2008). Monsoons as eddy-mediated regime transitions
382 of the tropical overturning circulation. *Nature Geoscience*, *11*, 515–519. doi:
383 10.1038/ngeo248
- 384 Cronin, T. W., & Jansen, M. F. (2016). Analytic radiative-advective equilibrium
385 as a model for high-latitude climate. *Geophysical Research Letters*, *43*(1), 449-
386 457. doi: 10.1002/2015GL067172
- 387 Crook, J. A., Forster, P. M., & Stuber, N. (2011). Spatial patterns of modeled
388 climate feedback and contributions to temperature response and polar amplifi-
389 cation. *Journal of Climate*, *24*(14), 3575-3592. doi: 10.1175/2011JCLI3863.1
- 390 Dai, A., Luo, D., Song, M., & Liu, J. (2019). Arctic amplification is caused by sea-
391 ice loss under increasing CO₂. *Nature Communications*, *10*(121). doi: 10.1038/
392 s41467-018-07954-9
- 393 Feldl, N., Bordoni, S., & Merlis, T. M. (2017). Coupled high-latitude climate feed-
394 backs and their impact on atmospheric heat transport. *Journal of Climate*,
395 *30*(1), 189-201. doi: 10.1175/JCLI-D-16-0324.1
- 396 Feldl, N., & Roe, G. H. (2013). Four perspectives on climate feedbacks. *Geophysical*
397 *Research Letters*, *40*(15), 4007-4011. doi: 10.1002/grl.50711
- 398 Flannery, B. P. (1984). Energy balance models incorporating transport of thermal
399 and latent energy. *Journal of the Atmospheric Sciences*, *41*(3), 414-421. doi:
400 10.1175/1520-0469(1984)041<0414:EBMITO>2.0.CO;2
- 401 Frierson, D. M. W., & Hwang, Y.-T. (2012). Extratropical influence on ITCZ shifts
402 in slab ocean simulations of global warming. *Journal of Climate*, *25*(2), 720-
403 733. doi: 10.1175/JCLI-D-11-00116.1
- 404 Goosse, H., Kay, J. E., Armour, K. C., Bodas-Salcedo, A., Chepfer, H., Docquier,
405 D., ... Vancoppenolle, M. (2018). Quantifying climate feedbacks in polar
406 regions. *Nature Communications*, *9*(1919). doi: 10.1038/s41467-018-04173-0
- 407 Graverson, R. G., & Wang, M. (2009). Polar amplification in a coupled climate
408 model with locked albedo. *Climate Dynamics*, *33*(5), 629–643. doi: 10.1007/
409 s00382-009-0535-6
- 410 Gregory, J. M., Ingram, W. J., Palmer, M. A., Jones, G. S., Stott, P. A., Thorpe,
411 R. B., ... Williams, K. D. (2004). A new method for diagnosing radiative

- 412 forcing and climate sensitivity. *Geophysical Research Letters*, *31*(3), L03205.
413 doi: 10.1029/2003GL018747
- 414 Hall, A. (2004). The role of surface albedo feedback in climate. *Journal of Climate*,
415 *17*(7), 1550-1568. doi: 10.1175/1520-0442(2004)017<1550:TROSAF>2.0.CO;2
- 416 Henry, M., & Merlis, T. M. (2019). The role of the nonlinearity of the ste-
417 fan-boltzmann law on the structure of radiatively forced temperature change.
418 *Journal of Climate*, *32*(2), 335-348. doi: 10.1175/JCLI-D-17-0603.1
- 419 Hwang, Y.-T., & Frierson, D. M. W. (2010). Increasing atmospheric poleward en-
420 ergy transport with global warming. *Geophysical Research Letters*, *37*(24),
421 L24807. doi: 10.1029/2010GL045440
- 422 Hwang, Y.-T., Frierson, D. M. W., & Kay, J. E. (2011). Coupling between arc-
423 tic feedbacks and changes in poleward energy transport. *Geophysical Research*
424 *Letters*, *38*(17), L17704. doi: 10.1029/2011GL048546
- 425 Jones, J. M., Gille, S. T., Goosse, H., Abram, N. J., Canziani, P. O., Charman,
426 D. J., ... Vance, T. R. (2016). Assessing recent trends in high-latitude South-
427 ern Hemisphere surface climate. *Nature Climate Change*, *6*, 917-926. doi:
428 10.1038/NCLIMATE3103
- 429 Merlis, T. M. (2014). Interacting components of the top-of-atmosphere energy bal-
430 ance affect changes in regional surface temperature. *Geophysical Research Let-*
431 *ters*, *41*, 7291-7297. doi: 10.1002/2014GL061700
- 432 Merlis, T. M., & Henry, M. (2018). Simple estimates of polar amplification in moist
433 diffusive energy balance models. *Journal of Climate*, *31*(15), 5811-5824. doi:
434 10.1175/JCLI-D-17-0578.1
- 435 Myhre, G., Shindell, D., Bréon, F.-M., Collins, W., Fuglestedt, J., Huang, J., ...
436 Zhang, H. (2013). Anthropogenic and natural radiative forcing [Book Sec-
437 tion]. In T. Stocker et al. (Eds.), *Climate Change 2013: The Physical Science*
438 *Basis. Contribution of Working Group I to the Fifth Assessment Report of*
439 *the Intergovernmental Panel on Climate Change* (p. 659-740). Cambridge,
440 United Kingdom and New York, NY, USA: Cambridge University Press. doi:
441 10.1017/CBO9781107415324.018
- 442 North, G. R., Cahalan, R. F., & Coakley Jr., J. A. (1981). Energy balance
443 climate models. *Reviews of Geophysics*, *19*(1), 91-121. doi: 10.1029/
444 RG019i001p00091

- 445 O’Gorman, P. A., & Schneider, T. (2008). The hydrological cycle over a wide range
446 of climates simulated with an idealized GCM. *Journal of Climate*, *21*(15),
447 3815-3832. doi: 10.1175/2007JCLI2065.1
- 448 Payne, A. E., Jansen, M. F., & Cronin, T. W. (2015). Conceptual model analysis of
449 the influence of temperature feedbacks on polar amplification. *Geophysical Re-*
450 *search Letters*, *42*(21), 9561-9570. doi: 10.1002/2015GL065889
- 451 Pithan, F., & Mauritsen, T. (2014). Arctic amplification dominated by temper-
452 ature feedbacks in contemporary climate models. *Nature Geoscience*, *7*, 181–
453 184. doi: 10.1038/NGEO2071
- 454 Roe, G. H., Feldl, N., Armour, K. C., Hwang, Y.-T., & Frierson, D. M. (2015). The
455 remote impacts of climate feedbacks on regional climate predictability. *Nature*
456 *Geoscience*, *8*, 135–139. doi: 10.1038/NGEO2346
- 457 Rose, B. E. J., Armour, K. C., Battisti, D. S., Feldl, N., & Koll, D. D. B. (2014).
458 The dependence of transient climate sensitivity and radiative feedbacks on the
459 spatial pattern of ocean heat uptake. *Geophysical Research Letters*, *41*(3),
460 1071-1078. doi: 10.1002/2013GL058955
- 461 Shaw, T. A., & Tan, Z. (2018). Testing latitudinally dependent explanations of
462 the circulation response to increased CO₂ using aquaplanet models. *Geophysi-*
463 *cal Research Letters*, *45*(18), 9861-9869. doi: 10.1029/2018GL078974
- 464 Shell, K. M., Kiehl, J. T., & Shields, C. A. (2008). Using the radiative kernel tech-
465 nique to calculate climate feedbacks in ncar’s community atmospheric model.
466 *Journal of Climate*, *21*(10), 2269-2282. doi: 10.1175/2007JCLI2044.1
- 467 Siler, N., Roe, G. H., & Armour, K. C. (2018). Insights into the zonal-mean re-
468 sponse of the hydrologic cycle to global warming from a diffusive energy
469 balance model. *Journal of Climate*, *31*(18), 7481-7493. doi: 10.1175/
470 JCLI-D-18-0081.1
- 471 Soden, B. J., Held, I. M., Colman, R., Shell, K. M., Kiehl, J. T., & Shields, C. A.
472 (2008). Quantifying climate feedbacks using radiative kernels. *Journal of*
473 *Climate*, *21*(14), 3504-3520. doi: 10.1175/2007JCLI2110.1
- 474 Stevens, B., Bony, S., & Webb, M. (2012). *Clouds on-off climate intercomparison*
475 *experiment (COOKIE)*. ([Available online at [https://pure.mpg.de/rest/](https://pure.mpg.de/rest/items/item_2078839/component/file_2079076/content)
476 [items/item_2078839/component/file_2079076/content](https://pure.mpg.de/rest/items/item_2078839/component/file_2079076/content)])
- 477 Stuecker, M. F., Bitz, C. M., Armour, K. C., Proistosescu, C., Kang, S. M.,

- 478 Xie, S.-P., . . . Jin, F.-F. (2018). Polar amplification dominated by lo-
479 cal forcing and feedbacks. *Nature Climate Change*, 8, 1076–1081. doi:
480 10.1038/s41558-018-0339-y
- 481 Taylor, K. E., Crucifix, M., Braconnot, P., Hewitt, C. D., Doutriaux, C., Broccoli,
482 A. J., . . . Webb, M. J. (2007). Estimating shortwave radiative forcing and
483 response in climate models. *Journal of Climate*, 20(11), 2530–2543. doi:
484 10.1175/JCLI4143.1
- 485 Taylor, K. E., Stouffer, R. J., & Meehl, G. A. (2012). An overview of CMIP5 and
486 the experiment design. *Bulletin of the American Meteorological Society*, 93(4),
487 485–498. doi: 10.1175/BAMS-D-11-00094.1
- 488 Turner, J., Hosking, J. S., Bracegirdle, T. J., Marshall, G. M., & Phillips, T. (2015).
489 Recent changes in Antarctic sea ice. *Philosophical Transactions of the Royal*
490 *Society A*, 373, 20140163. doi: 10.1098/rsta.2014.0163
- 491 Vavrus, S. (2004). The impact of cloud feedbacks on arctic climate under greenhouse
492 forcing. *Journal of Climate*, 17(3), 603–615. doi: 10.1175/1520-0442(2004)
493 017<0603:TIOCFO>2.0.CO;2
- 494 Voigt, A., Biasutti, M., Scheff, J., Bader, J., Bordoni, S., Codron, F., . . . Var-
495 gas Zeppetello, L. R. (2016). The tropical rain belts with an annual cycle and
496 a continent model intercomparison project: TRACMIP. *Journal of Advances*
497 *in Modeling Earth Systems*, 8(4), 1868–1891. doi: 10.1002/2016MS000748